ARTICLE

OBC
www.rsc.org/obc

Structure, modelling and dynamic behaviour of aza- and azaoxamacrocyclic ligands derived from (*R*,*R*)-1,2-diaminocyclohexane †

Sonia Pulacchini, Rima Nasser, Kevin F. Sibbons, Majid Motevalli, Geoffrey E. Hawkes, Romano T. Kroemer,‡ Edson S. Bento § and Michael Watkinson *

Department of Chemistry, Queen Mary, University of London, Mile End Road, London, UK E1 4NS. E-mail: m.watkinson@qmul.ac.uk

Received 23rd June 2003, Accepted 9th September 2003
First published as an Advance Article on the web 2nd October 2003

Investigations into the conformational behaviour of macrocyclic ligands **5** and **6** derived from (*R*,*R*)-1,2-diaminocyclohexane have been undertaken using molecular modelling, single crystal X-ray diffraction and variable temperature ^{1}H NMR spectroscopy. These have revealed that the lowest energy conformers in both cases do not possess the expected C_2-element of symmetry, which can only be accessed at higher temperatures. Instead both molecules exist as C_1-conformers at room temperature and in the solid state. In solution a range of dynamic exchange processes is observed which result, in part from the inherent strain in these fused bicyclic systems. An unexpected but characteristic feature of the C_1-symmetric conformers is highlighted by the presence of a signal at unexpectedly low field in their ^{1}H NMR spectra due to the interaction of two of the sulfonyl oxygen atoms with one of the bridgehead hydrogen atoms.

Introduction

We have recently become interested in the synthesis of novel enantiomerically pure analogues of the macrocyclic ligand 1,4,7-triazacyclononane, **1**, using classical synthetic methodology due to the catalytic activity that a number of its transition metal complexes have shown.[1] These catalytic processes cover a diverse range of synthetically useful transformations, which although mainly oxidative in nature, also include the hydrolytic cleavage of activated phosphate esters, RNA and DNA.[2] In all of our efforts towards such ligands we have thus far attempted to include the important C_2-element of symmetry within the macrocyclic framework, with an ultimate aim of generating modular structures like **2** and **3**, which, until very recently,[3,4] had not been reported. The vicinal diamine 1,2-diaminocyclohexane appeared to be an ideal starting point for these investigations, as both enantiomers are readily available and there was good precedent for this backbone acting as an excellent chiral reporter in asymmetric catalysis, most notably in Jacobsen's applications of metallo-salen complexes.[5] We therefore began our investigations with the generic structure **4** as a synthetic target. At the outset of these investigations one report of this ligand structure had appeared in a patent,[3a] however, the synthesis of a number of 'sandwich' complexes of **4** subsequently appeared.[3b] Despite extensive attempts, the reported procedures proved unsatisfactory in our hands. We therefore investigated alternative synthetic strategies and found that we could isolate **5**, a key intermediate in the synthesis of **4**, in a modest yield of 46%.[1a] We were able to improve the yield of its azaoxa-analogue **6** to 62%, and postulated that the inherent ring strain in **5**, due to the fused bicyclic system containing three essentially planar sp^2 hybridised nitrogen atoms, was the cause. In addition the room temperature ^{1}H NMR of both **5** and **6** revealed some unexpected features.

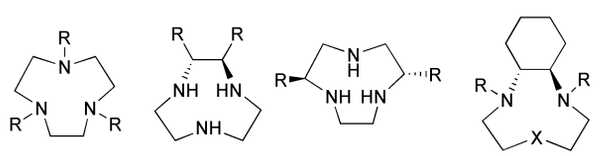

1 **2** **3**

4 R = H, X = NH
5 R = Ts, X = NTs
6 R = Ts, X = O

In both systems it was apparent that a number of dynamic exchange processes were occurring and that the lowest energy structures were not C_2-symmetric. Furthermore in both cases an unexpected ^{1}H signal appeared around 5 ppm which was difficult to account for in structures **5** and **6**. We therefore decided to undertake a detailed structural solid and solution state analysis of these macrocycles using molecular modelling, single crystal X-ray diffraction and VT-NMR in an attempt to better understand this behaviour.

Results and discussion

Our initial investigations involved the more straightforward azaoxamacrocyclic system **6**, which, due to its reduced structural complexity, we hoped would simplify the initial analysis of VT-NMR (variable temperature NMR) spectra and reduce the length of the theoretical calculations. The single crystal X-ray structure of **6** revealed that two macrocycles and a water molecule are present in the asymmetric unit, the water molecule acting as a bridge between the two virtually identical macrocycles, Figs. 1 and 2. One hydrogen atom of the water molecule interacts *via* a hydrogen bond with oxygen atom O(10) of one macrocyclic ring, whilst the second hydrogen atom of the water molecule interacts with the sulfonamide groups of the other macrocycle *via* hydrogen bonds with O(1) and O(3), Fig. 1.

Although all bond lengths and angles are unexceptional and the cyclohexane ring shows an ideal chair conformation with the two *trans*-nitrogen substituents in equatorial positions, two features are immediately evident from the crystal structure of **6**, the first being that the structure does not possess C_2-symmetry. The second important observation is the very different environments of H(19) and H(20), Fig. 2, which provides an

† Electronic supplementary information (ESI) available: different views of compounds **6**, **6a** and **6b**. See http://www.rsc.org/suppdata/ob/b3/b306963j/

‡ Present address: Molecular Modeling & Design, Pharmacia, Viale Pasteur 10, 20014 Nerviano (MI) – Italy

§ Present address: Departamento de Química, Universidade Federal de Alagoas, Maceió, AL, Brazil, 57.072-970.

DOI: 10.1039/b306963j

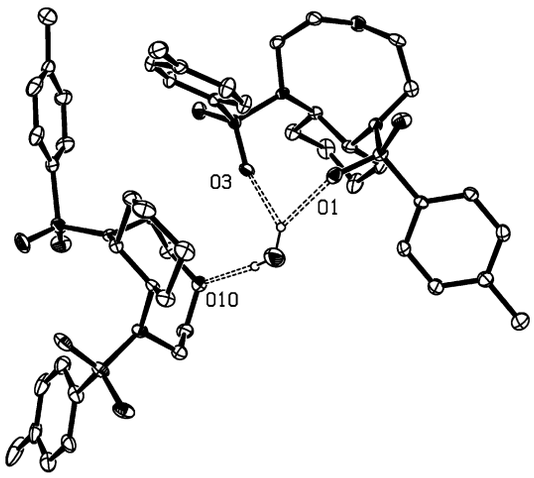

Fig. 1 ORTEP plot of the single crystal X-ray structure of **6** showing the hydrogen bonded dimer with hydrogen bond distances (Å) and e.s.ds. O(11)–H(11A) ··· O(1) 2.845(8), O(11)–H(11A) ··· O(3) 3.086(7), O(11)–H(11B) ··· O(10) 2.869(8).

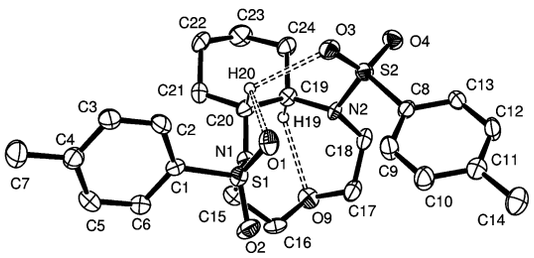

Fig. 2 ORTEP plot of one of the molecules of **6** found in the asymmetric unit showing the interactions of the hydrogen attached to the carbon bridgeheads with the sulfonamide and macrocyclic oxygen atoms. All hydrogen atoms with the exception of H(19) and H(20) have been omitted for clarity. Selected bond angles (°) with e.s.ds. N(1)–S(1)–C(1) 110.6(2), C(20)–N(1)–C(15) 120.3(5), C(20)–N(1)–S(1) 118.8(4), C(15)–N(1)–S(1) 116.9(4), N(1)–C(20)–C(19) 111.0(5), N(1)–C(20)–C(21) 112.4(5), N(2)–S(2)–C(8) 102.8(2), C(18)–N(2)–C(19) 116.2(4), C(19)–N(2)–S(2) 118.3(4), C(18)–N(2)–S(2) 114.5(4), N(2)–C(19)–C(20) 112.3(4), N(2)–C(19)–C(24) 113.9(5).

explanation for the signal at unexpectedly low field (4.78–5.02 ppm) in the ^{1}H-NMR spectra. As can be seen in Fig. 2, H(20) interacts strongly with two of the oxygen atoms of the sulfonamide groups H(20)–O(1) = 2.471 Å and H(20)–O(3) = 2.412 Å, accounting for the low field signal observed in the ^{1}H NMR spectrum (*vide infra*). In contrast H(19) is in a completely different environment and only interacts with O(9) of the macrocyclic ring (O(9)–H(19) = 2.445 Å).

The crystal structure of **6** proved valuable as it served as a starting geometry for the *ab initio* calculations,[6,7] which were used to estimate the energy difference between the C_1- and any C_2-symmetric conformations. The X-ray structure was subsequently optimised in order to give the modelled C_1-symmetric conformer, and as a result of the quantum chemical calculations two additional C_2-symmetric conformers were identified and their calculated relative energies are listed in Fig. 3.

The structure of the optimised C_1-symmetric conformer is given in Fig. 3 (see also supplementary information †). It can be clearly seen that the sulfonamide groups have different spatial orientations and it is as expected very similar to the structure obtained by single crystal diffraction. The cyclohexane ring hardly deviates from the ideal chair conformation as in the crystal structure. Similarly, the hydrogen atoms attached to the carbon bridgeheads are situated in very different environments. One of these hydrogens is very close to one oxygen of both sulfonamide groups. The corresponding O ··· H distances are 2.35 and 2.26 Å which are a little shorter than those measured in the crystal structure (2.471 and 2.412 Å). The only interaction of the hydrogen atom attached to the second carbon

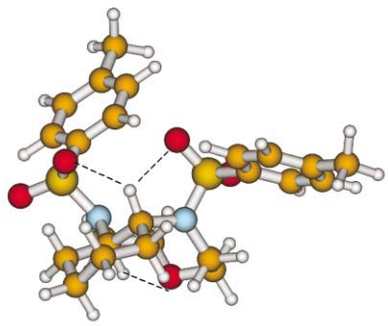

Conformer	*Relative energy (kJ mol^{-1})*
C_1-**6**	0
C_2-**6a**	109.307
C_2-**6b**	116.060

Fig. 3 The interactions of the hydrogen atoms attached to the carbon bridgeheads with oxygen atoms in **6**. The relative energies of the three conformers calculated with the GAUSSIAN98 program[6] carried out at the Hartree–Fock level of theory using a 3-21G* basis set.[7]

bridgehead is with the ring oxygen at a distance of 2.22 Å, which is again a rather shorter distance compared to the single crystal structure (2.445 Å). The apparent compactness of this optimised structure can be at least partially attributed to the "*in-vacuo*" treatment of the molecule during optimisation.

The two C_2-symmetric conformers are similar to one another, differing only slightly in the spatial orientation of the tosyl groups, as shown in Fig. 4 (see also supplementary information †). The much higher energy of these C_2-symmetric conformers compared to the C_1-symmetric conformer appears to be caused by geometric strain. In the C_2-symmetric conformers the cyclohexane ring does not retain the ideal chair conformation (see Fig. 4 and supplementary information †) seen in both the C_1-symmetric conformer and the single crystal X-ray structure, with the geometry of the carbon bridgeheads being particularly distorted. This high degree of strain is consistent with the high temperature required in the NMR studies to achieve a C_2-symmetric conformer in solution (*vide infra*). It is also interesting that the distances of the axial hydrogen atoms attached to the carbon bridgeheads and the oxygen atoms of the sulfonamide groups are calculated to be 2.48 and 3.60 Å. This indicates that, in the C_2-symmetric conformation, these hydrogen atoms interact strongly with only one oxygen donor in

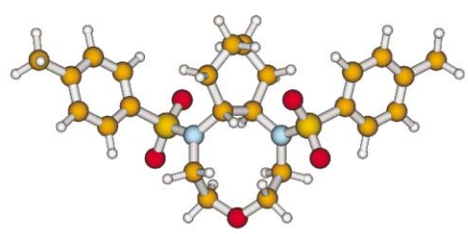

Conformer C_2-**6a**

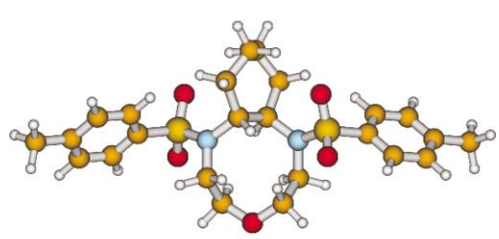

Conformer C_2-**6b**

Fig. 4 Structures of the two C_2-symmetric conformers of **6** obtained by molecular modelling.

contrast to the situation observed for the C_1-confomer. This structural information is essential in order to understand the unexpectedly complex solution behaviour of **6** as revealed in its room temperature ^{1}H-NMR spectrum. This spectrum, Fig. 5, clearly shows that the molecule is not C_2-symmetric and that exchange processes are occurring, as judged by the broad signals observed at various temperatures. The X-ray structure and molecular modelling are particularly useful for the analysis of this behaviour and the lower energy C_1-symmetric conformer was assumed to be the lowest energy solution structure in our analysis which allows us to readily assign the unexpected signal between 4.78 and 5.02 ppm to H(20) as a result of the interactions with O(1) and O(3).

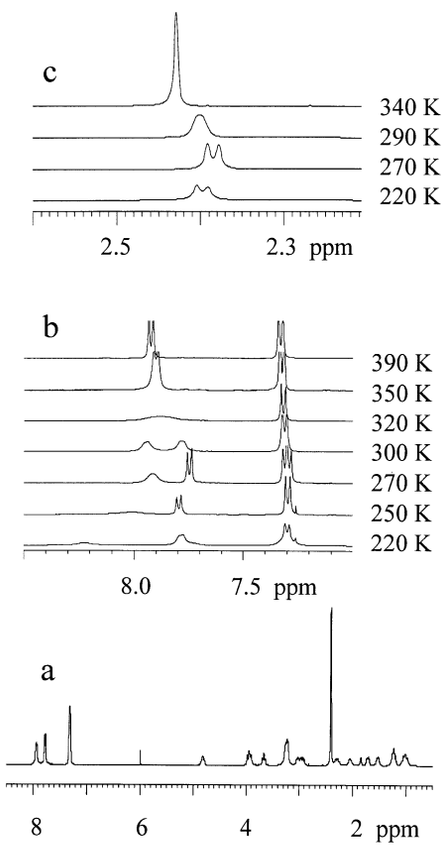

Fig. 5 400 MHz ^{1}H NMR spectra of **6**, (a) full spectrum at 300 K; (b) variable temperature spectra of the aromatic region; (c) variable temperature spectra of the methyl region.

The dynamic solution behaviour of **6** was then investigated by variable temperature ^{1}H-NMR. The temperature dependence of the aromatic region of the ^{1}H-NMR spectrum of **6** is shown in Fig. 5b. At the highest temperature (390 K) the spectrum is relatively simple with the protons *ortho*- to the sulfonamide group giving the doublet at 7.90 ppm, and the *meta*- protons the doublet at 7.30 ppm. As the temperature is decreased it is clear that two distinct dynamic processes affect the spectrum. The process with the higher temperature coalescence separates the *ortho*- signal (coalescence at *ca.* 320 K) into two signals at 7.82 and 7.98 ppm (see spectrum at 300 K), and the *meta*- signal (coalescence at *ca.* 290 K) into two overlapping doublets (apparent triplet at 270 K). The process with the lower temperature coalescence principally affects the *ortho*- doublet at 7.98 ppm, which has a coalescence at *ca.* 240 K, separating into two broad signals at 7.72 and 8.23 ppm. This second dynamic process does not affect the appearance of the *meta*- proton signal, as the two *meta*- doublets appear to have identical chemical shifts in the temperature range 220 to 260 K. At the lowest temperature (220 K) the *ortho*- doublet at 7.82 ppm exhibits some broadening which may indicate the onset of a slowing of a possible third dynamic process.

It is known[8] that sulfonamides can exhibit two distinct dynamic processes, one is hindered (amide-like) rotation about the N–S bond, and the other is slow inversion at pyramidal nitrogen. However, the nitrogen of the sulfonamide group is often planar or near planar, and therefore the inversion process is not relevant. In the present case the X-ray structure reveals that the two nitrogen atoms in this low energy C_1-conformer are almost planar with the sum of the bond angles at each of the two nitrogens of 352° and 353°. Therefore only the hindered rotation about the N–S bond need be considered.

The dynamic process is easily visualised as arising from some double bond character between nitrogen and sulfur. A planar, or near planar nitrogen atom, requires a contribution of a canonical form in which it can be considered to be sp^2 hybridised. This implies considerable double bond character between the nitrogen and sulfur atoms, a consequence of which is an increased barrier to rotation about the N–S bond resulting in hindered rotation.

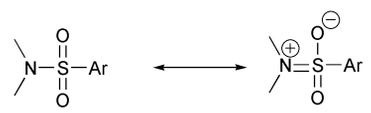

A ***B***

As the sulfur atom is effectively tetrahedral (as seen in the X-ray structure), such hindered rotation will generate two environments for the aromatic ring if the molecule does not possess a plane of symmetry which includes the trigonal nitrogen plane of canonical form B:

Therefore the spectrum at 220 K is consistent with the C_1-symmetric structure having two different tosyl environments (pseudo-axial and pseudo-equatorial), with one of these environments exhibiting slow N–S bond rotation (*ortho*- signals at 7.72 and 8.23 ppm), whereas the other environment exhibits relatively rapid N–S bond rotation (*ortho*- signal at 7.82 ppm). As the temperature is increased, enhanced N–S bond rotation coalesces the separate *ortho*- signals for one tosyl environment. Further increase in temperature then coalesces the *ortho*- signals for the two different tosyl environments. The mechanism for this higher temperature equilibration is most likely to be a conformational change in the 9-membered ring which interconverts the pseudo-axial and pseudo-equatorial tosyl environments rather than nitrogen inversion for the reasons already presented (*vide supra*).

For the higher temperature dynamic process, the *ortho*- proton signal band-shapes (see Experimental Section) were analysed and yielded pseudo first order rate coefficients (k) in the range 28 s^{-1} at 300 K to 615 s^{-1} at 340 K (see Table 1). The plots of $\ln(k)$ *vs.* T^{-1} (Arrhenius) and $\ln(k/T)$ *vs.* T^{-1} (Eyring) were both linear. The Arrhenius plot gave a value for the activation energy E_a = 65.2 kJ mol^{-1} and Arrhenius A-factor = 6.5×10^{12}, and the Eyring plot gave a value for the activation enthalpy, ΔH^* = 62.5 kJ mol^{-1} and activation entropy, ΔS^* = -8.5 J K^{-1} mol^{-1}. The Eyring parameters give the free energy of activation ΔG^* = 64.8 kJ mol^{-1} at 273 K.

For the lower temperature dynamic process, separation of two *ortho*- signals for one of the tosyl environments was similarly analysed, and rates varied from 75 s^{-1} at 220 K to 799 s^{-1} at 250 K (see Table 1). The Arrhenius and Eyring plots were both linear, and gave E_a = 37.2 kJ mol^{-1} and Arrhenius A-factor = 5.7×10^{10}, and ΔH^* = 65.8 kJ mol^{-1} and ΔS^* =

Table 1 Rate coefficients for compound **6** from NMR bandshape analysis

	k/s^{-1}	
T/K	Ar[a]	Me[b]
220	75	
230	219	
240	579	0.01
250	799	0.04
260		0.18
270		0.98
280		2.4
290		8.4
300	28	31
310	72	
320	153	
330	321	
340	615	

[a] Bandshape analysis on ^{1}H signals in aromatic spectral region. [b] Bandshape analysis on ^{1}H Me signals.

94.3 J K^{-1} mol^{-1} respectively. The free energy of activation (ΔG^*) for N-inversion or N–S bond rotation of a tosyl derivative was determined to be 57.3 kJ mol^{-1} at 273 K.[9] The Eyring parameters derived above for the lower temperature dynamic process predict a value for the N–S bond free energy rotation barrier at 273 K, ΔG^* = 40.1 kJ mol^{-1}, which is of a similar magnitude to that reported.[9]

Analysis of the lower frequency, methyl group region of the temperature dependent ^{1}H-NMR spectra of **6** revealed that at lower temperatures there are two equally intense methyl singlets, which coalesce around 290 K, collapsing to a single signal at higher temperatures, Fig. 5c. Bandshape analysis gave the rates of the dynamic process (see Table 1), and the Eyring plot gave ΔH^* = 77.8 kJ mol^{-1} and ΔS^* = 42.0 J K^{-1} mol^{-1}, which gives the free energy of activation ΔG^* = 66.3 kJ mol^{-1} at 273 K. This value for ΔG^* is almost identical to that for the pseudo-axial to pseudo-equatorial interconversion determined from the *ortho*- proton bandshape analysis (64.8 kJ mol^{-1} at 273 K), and quite different to that for the hindered rotation about the N–S bond (40.1 kJ mol^{-1} at 273 K). The methine and methylene proton signals for **6**, in the region 0.9 to 5.0 ppm, were quite strongly overlapping and strongly temperature dependent, and no attempt was made to analyse these signals in detail.

Having established the cause of the complex dynamic solution behaviour of **6** an analogous approach was adopted for **5**. Although the chiral triazacyclononane ligand **5** was recently reported,[3b] no spectroscopic data were provided, perhaps as a result of its unexpectedly complex ^{1}H NMR spectrum at room temperature, Fig. 6a. As for **6**, it was immediately evident that the molecule is not C_2-symmetric and that all signals are broad indicating the presence of dynamic exchange processes. The unexpected but characteristic broad signal at 4.71–4.92 ppm is again present. In addition three distinct peaks (in the range between 2.3–2.4 ppm) can be distinguished for the methyl substituents of the sulfonamide groups.

The aromatic region of the ^{1}H NMR spectra of **5** as a function of the temperature is shown in Fig. 6b. At the highest temperature (390 K) there is a doublet at 7.92 ppm due to the four *ortho*- protons of the interconverting tosyl groups adjacent to the 6-membered ring, and a doublet at 7.62 ppm due to the two *ortho*- protons of the tosyl group remote from the carbon bridgeheads [N(2) in the crystal structure (*vide infra*)]. All of the *meta*- protons occur as two overlapping doublets around 7.32 ppm. As the temperature is decreased the signal at 7.92 ppm behaves in a similar manner to the *ortho*- proton signal for **6**. It first separates into two doublets (see spectrum at 300 K) at 7.80 and 7.98 ppm due to a slowing of the pseudo-axial and

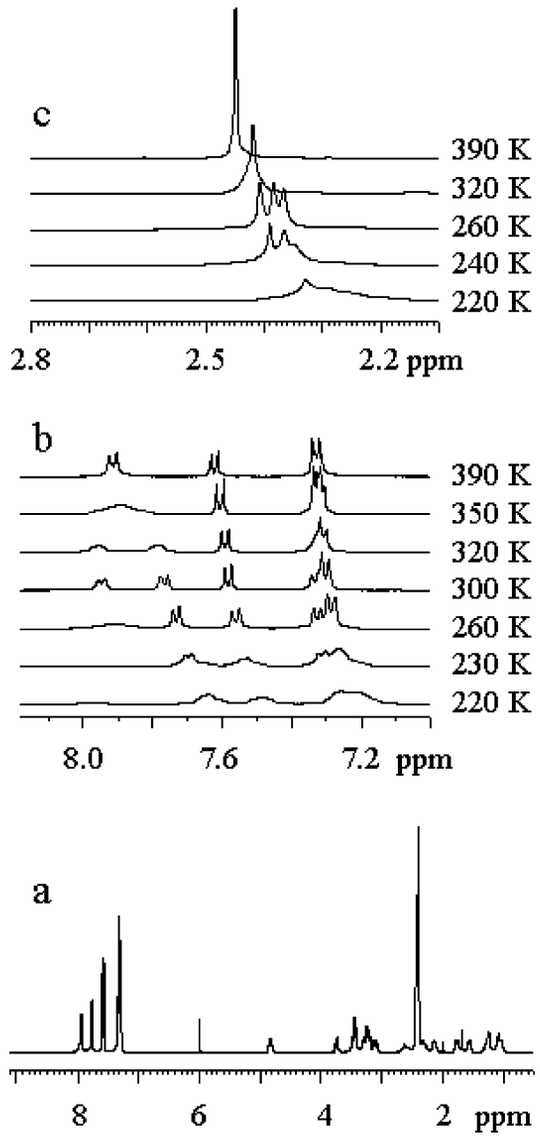

Fig. 6 400 MHz ^{1}H NMR spectra of **5**, (a) full spectrum at 300 K; (b) variable temperature spectra of the aromatic region; (c) variable temperature spectra of the methyl region.

pseudo-equatorial interchange. The higher frequency doublet then further separates into two broad signals, one apparent at about 8.10 ppm and the other part of the broad signal around 7.80 ppm, due to a slowing of the rotation about the N–S bond. At the lowest temperature (220 K) all other aromatic signals appear broadened, probably due to slow rotation about all N–S bonds.

The methyl region of the ^{1}H NMR spectra of **5** as a function of the temperature is shown in Fig. 6c. It can be seen that at the highest temperature (390 K) the two methyl signals, one from the rapidly interchanging pseudo-axial and pseudo-equatorial tosyl groups and the other from the tosyl group at N(2) are isochronous. As the temperature is decreased coalescence appears around 320 K and at 260 K three distinct methyl signals are seen at 2.44, 2.45 and 2.47 ppm. The signal at 2.45 ppm remains unchanged through this temperature range and is probably due to the tosyl group at N(2), whereas the other two signals are due to slowing of the pseudo-axial to pseudo-equatorial interchange. At 240 K the lowest frequency methyl signal is broadened, presumably due to slowing of the N–S bond rotation and at the lowest temperature (220 K) all methyl signals are broadened. The ^{1}H-NMR bandshapes from the aromatic region of **5** were analysed in the quantitative manner described previously for **6**, in the temperature range 300 to 390 K. The derived rate coefficients are given in Table 2.

Table 2 Rate coefficients for compound **5** from NMR bandshape analysis[a]

T/K	k/s^{-1}
300	10
320	20
350	120
390	170

[a] Bandshape analysis on ^{1}H signals in aromatic spectral region.

The Eyring plot was linear and gave the value $\Delta G^* = 64.3$ kJ mol^{-1} at 273 K, very similar to the values found for **6** for the pseudo-axial to pseudo-equatorial exchange process.

The comparable behaviour of **5** and **6** is further reinforced by the single crystal X-ray structure of **5**, Fig. 7. As for **6** the conformation of **5** in the crystal structure is C_1-symmetric with the cyclohexane ring again having a perfect chair conformation with C–C bonds between 1.508(8) and 1.523(9) Å. The N–S distances are typical for the tosyl group, although the N(3)–S(2) bond is slightly longer.[1a] The C–N distances are also typical apart from the N(3)–C(26) bond which is elongated. These slight distortions from optimal geometry are perhaps a result of the increased strain in this fused bicyclic structure compared to **6**, in which three essentially planar nitrogen atoms substituted with bulky tosyl groups must be accommodated. Herein lies the likely reason for the reduced yield of **5** compared to the respectable yield of **6**.

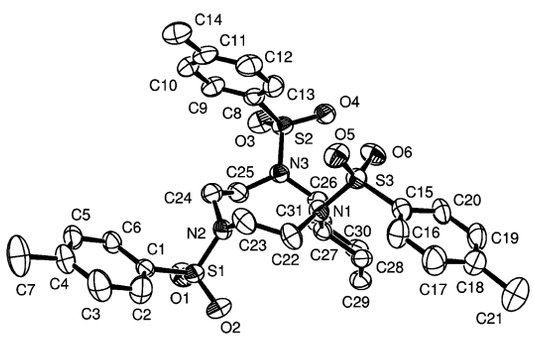

Fig. 7 ORTEP single crystal X-ray structure of **5** with selected bond lengths (Å) and angles (°) with e.s.ds. S(1)–N(2) 1.623(5), S(2)–N(3) 1.636(5), S(3)–N(1) 1.624(5), N(1)–C(22) 1.478(7), N(1)–C(27) 1.479(7), N(2)–C(23) 1.467(8), N(2)–C(24) 1.460(8), N(3)–C(25) 1.468(7), N(3)–C(26) 1.492(7); C(27)–N(1)–C(22) 114.6(4), C(27)–N(1)–S(3) 123.2(3), C(22)–N(1)–S(3) 116.5(4), N(1)–C(27)–C(26) 113.8(4), N(1)–C(27)–C(28) 114.4(5), N(1)–S(3)–C(15) 110.6(3), C(23)–N(2)–C(24) 119.2(5), C(23)–N(2)–S(1) 117.2(4), C(24)–N(2)–S(1) 118.5(5), N(2)–S(1)–C(1) 108.0(2), C(25)–N(3)–S(2) 115.0(4), C(25)–N(3)–C(26) 119.8(5), C(26)–N(3)–S(2) 118.2(3), N(3)–C(26)–C(27) 112.3(4), N(3)–C(26)–C(31) 112.5(5), N(3)–S(2)–C(8) 102.1(2).

Conclusion

The unexpected difficulties in the synthesis of these apparently simple macrocyclic ligands have been rationalised as a result of a thorough investigation into their conformational behaviour in the solid state, solution and also using theoretical calculations. The dynamic behaviour of these simple macrocyclic ligands in solution caused extensive problems during their characterisation and a rigorous understanding of their conformational behaviour has been achieved. This has allowed us to account for their challenging syntheses. The low yield obtained for the preparation of **5** can be explained in terms of geometric constraint. Since the structure of this macrocycle is extremely strained, ring closure is disfavoured. The more satisfactory synthesis of **6** probably results from the reduced strain when an oxygen atom replaces the cumbersome sulfonamide group in the macrocyclic structure, however, even in this case the bicyclic system remains relatively strained as is reflected in the dynamic NMR processes.

Experimental

The macrocyclic ligands **5** and **6** were prepared as previously described.[1a] Crystals of **5** suitable for single crystal X-ray diffraction studies were obtained by layering a dichloromethane solution of **5** with hexane whilst those of **6** were obtained by slow evaporation of an ethanolic solution.

Single crystal X-ray diffraction studies

Intensity data were collected on an Enraf-Nonius CAD-4 diffractometer using Mo-Kα radiation (λ = 0.71073 Å) with ω-2θ scans. Structures were solved by direct methods using the SHELXS-97 program[10] and developed by Fourier difference techniques with subsequent refinement on F^2 by full matrix least squares using SHELXL-97.[10] Absorption corrections were initially carried out by Ψ-scans[11] and later using the program DIFABS.[12] The hydrogen atoms on the water molecule were found in the difference map, but O–H distances were fixed at 0.85(2) Å during refinement. The positions of all other H-atoms were calculated geometrically and refined using an atom riding model. A restrained refinement of anisotropic thermal parameters was carried out for all non-hydrogen atoms. Publication material was prepared using WINGX[13] and molecular graphics using ORTEP-3.[14] Crystallographic data for **5** (CCDC 206545) and **6** (CCDC 206544) have been deposited at the Cambridge Crystallographic Data Centre. See http://www.rsc.org/suppdata/ob/b3/b306963j/ for crystallographic data in .cif or other electronic format.

Crystal data for **5**. $C_{31}H_{39}N_3O_6S_3$, M = 645.83, orthorhombic, a = 22.981(3), b = 13.623(3), c = 10.142(2) Å, U = 3175.2(10) Å^3, T = 293(2) K, space group $P2_12_12_1$, Z = 4, μ(Mo–K$_\alpha$) = 0.281 mm^{-1}, 3231 reflections measured, 3142 unique (R_{int} = 0.0049) which were used in all calculations. The final R [I>2σ(I)] was 0.0402 and wR = 0.1085.

Crystal data for **6**. $C_{24}H_{33}N_2O_{5.50}S_2$, M = 501.64, monoclinic, a = 14.905(8), b = 17.292(3), c = 9.515(2) Å, β = 93.09(2) °, U = 2448.8(15) Å^3, T = 160(2) K, space group $P2_1$, Z = 4, μ(Mo–K$_\alpha$) = 0.258 mm^{-1}, 4888 reflections measured, 4461 unique (R_{int} = 0.0155) which were used in all calculations. The final R [I>2σ(I)] was 0.0461 and wR = 0.0987.

Molecular modelling

Quantum chemical calculations with the GAUSSIAN98 program[6] were carried out at the Hartree–Fock level of theory using a 3-21G* basis set.[7] Previous studies have demonstrated that such calculations produce accurate estimates for relative energies and rotation barriers in diarylacenaphthene systems.[15] Full geometry optimisations were performed for three conformers of **6**. Two of these optimisations were carried out on C_2-symmetric conformers of **6**. For the third geometry optimisation (the C_1-symmetric conformer) the crystal structure of **6** served as the starting geometry.

VT-NMR

For the variable temperature experiments, all NMR spectra were measured at 400 MHz using a Bruker AMX-400 spectrometer. The temperature controller was calibrated against a standard methanol sample, and reported temperatures are believed to be accurate to ± 1°. The simulations of the spectral bandshapes were performed on a PC using the Bruker *WINDYNA* software.[16] Samples were contained in 5 mm o.d. tubes, and *ca.* 5 mg compound was dissolved in 0.5 ml of $C_2D_2Cl_4$.

Acknowledgements

We are grateful to Queen Mary, University of London for a studentship (SP), to the EPSRC for financial support (RN GR/98700139 and KFS, GR/R19182/01), and to the CNPq for

a fellowship (ESB). We are indebted to The University of London Intercollegiate Research Service for ^{1}H NMR spectra at 400 MHz (Queen Mary). We also thank The University of London Central Research Fund, The Nuffield Foundation and The Royal Society for financial support.

References

1 (*a*) S. Pulacchini, K. F. Sibbons, K. Shastri, M. Motevalli, M. Watkinson, H. Wan, A. Whiting and A. P. Lightfoot, *J. Chem. Soc., Dalton Trans.*, 2003, 2043; (*b*) J. E. W. Scheurmann, F. Ronketti, M. Motevalli, D. V. Griffiths and M. Watkinson, *New. J. Chem.*, 2002, **26**, 1054–1059; (*c*) J. S. Bradshaw, Aza-crown macrocycles, Wiley, New York, 1993.

2 See for example (*a*) E. L. Hegg and J. N. Burstyn, *Coord. Chem. Rev.*, 1998, **173**, 133; (*b*) N. H. Williams, B. Takasaki, M. Wall and J. Chin, *Acc. Chem. Res.*, 1999, **32**, 485; (*c*) M. J. Young and J. Chin, *J. Am. Chem. Soc.*, 1995, **117**, 10577; (*d*) B. R. Bodsgard and J. N. Burstyn, *Chem. Commun.*, 2001, 647.

3 (*a*) M. Beller, A. Tafesch, R. W. Fischer and B. Scharbert, DE 19523891, 1995; (*b*) S. W. Golding, T. W. Hambley, G. A. Lawrance, S. M. Luther, M. Maeder and P. Turner, *J. Chem. Soc., Dalton Trans.*, 1999, 1975.

4 (*a*) G. Argouarch, C. L. Gibson, G. Stones and D. C. Sherrington, *Tetrahedron Lett.*, 2002, **43**, 3795; (*b*) B. M. Kim, S. M. So and H. J. Choi, *Org. Lett.*, 2002, **4**, 949.

5 See for example (*a*) E. N. Jacobsen, *Comprehensive Asymmetric Catalysis*, Volume II, Chapter 17, p 607; (*b*) E. N. Jacobsen and M. H. Wu, *Comprehensive Asymmetric Catalysis*, Volume II, Chapter 18.2, p 649; E. N. Jacobsen and M. H. Wu, *Comprehensive Asymmetric Catalysis*, Volume III, Chapter 35, p 1309, Ed. E. N. Jacobsen, A. Pfaltz and H. Yamamoto, Springer-Verlag, Berlin-Heidleberg-New York, 1999.

6 M. J. Frisch, G. W. Trucks, H. B. Schlegel, G. E. Scuseria, M. A. Robb, J. R. Cheeseman, V. G. Zakrzewski, J. A. Montgomery, Jr., R. E. Stratmann, J. C. Burant, S. Dapprich, J. M. Millam, A. D. Daniels, K. N. Kudin, M. C. Strain, O. Farkas, J. Tomasi, V. Barone, M. Cossi, R. Cammi, B. Menucci, C. Pomelli, C. Adamo, S. Clifford, J. Ochterski, G. A. Petersson, P. Y. Ayala, Q. Cui, K. Morokuma, D. K. Malick, A. D. Rabuck, K. Raghavachari, J. B. Foresman, J. Cioslowski, J. V. Ortiz, A. G. Baboul, B. B. Stefanov, G. Liu, A. Liashenko, P. Piskorz, I. Komaromi, R. Gomperts, R. L. Martin, D. J. Fox, T. Keith, M. A. Al-Laham, C. Y. Peng, A. Nanayakkara, C. Gonzalez, M. Challacombe, P. M. W. Gill, B. Johnson, W. Chen, M. W. Wong, J. L. Andres, C. Gonzalez, M. Head-Gordon, E. S. Replogle and J. A. Pople, *Gaussian 98, Revision A.7*; Gaussian, Inc.: Pittsburgh, PA, 1998.

7 J. S. Binkley, J. A. Pople and W. J. Hehre, *J. Am. Chem. Soc.*, 1980, **102**, 939.

8 See for example (*a*) J. B. Nicholas, R. Vance, E. Martin, B. J. Burke and A. J. Hopfinger, *J. Phys. Chem.*, 1991, **95**, 9803; (*b*) J. Heyd, W. Thiel and W. Weber, *Theochem. J. Mol. Struct.*, 1997, **391**, 125.

9 D. Crich, M. Bruncko, S. Natarajan, B. K. Teo and D. A. Tocher, *Tetrahedron*, 1995, **51**, 2215.

10 G. M. Sheldrick, SHELX-97 Program for Solution and Refinement of Crystal Structures . University of Göttingen, Germany, 1997.

11 A. C. T. North, D. C. Phillips and F. S. Mathews, *Acta Crystallogr., Sect. A*, 1968, **24**, 351.

12 N. Walker and D. Stuart, *Acta. Crystallogr., Sect. A*, 1983, **39**, 158.

13 L. J. Farrugia, WinGX- A Windows Program for Crystal Structure Analysis, University of Glasgow, Glasgow, 1998.

14 L. J. Farrugia, ORTEP-3 for Windows. J. Appl. Crystallogr., 1997, **30**, 565.

15 W. Cross, G. E. Hawkes, R. T. Kroemer, K. R. Liedl, T. Loerting, R. Nasser, R. G. Pritchard, M. Steele, M. Watkinson and A. Whiting, *J. Chem. Soc., Perkin Trans 2*, 2001, 459.

16 T. Lenzen and G. Haggle, WINDYNA 32, version 1.01; Bruker Analytik Gmbh, 1998.